Evidence for internal stresses induced by nanoimprint lithography

Hyun Wook Ro, Yifu Ding, and Hae-Jeong Lee
NIST Polymers Division, 100 Bureau Drive, Gaithersburg, Maryland 20899-8541

Daniel R. Hines
Laboratory for Physical Sciences, University of Maryland, 8050 Greenmead Drive, College Park, Maryland 20740

Ronald L. Jones, Eric K. Lin, Alamgir Karim, Wen-li Wu, and Christopher L. Soles[a)]
NIST Polymers Division, 100 Bureau Drive, Gaithersburg, Maryland 20899-8541

(Received 15 June 2006; accepted 9 October 2006; published 30 November 2006)

The thermal embossing form of nanoimprint lithography is used to pattern arrays of nanostructures into three different polymer films. The shape of the imprinted patterns is characterized with nanometer precision using both x-ray scattering and reflectivity techniques. The time dependent response of the pattern shape at temperatures near the glass transition temperature reveals large levels of residual stress induced by the imprinting process. During the imprint, large shear fields are generated as the viscous polymer flows into the mold. If these shear distortions do not have time to relax during the imprinting, internal stresses are frozen into the final pattern. At elevated temperatures in the freestanding structures (once the mold has been separated from the imprint), there is an accelerated reduction in pattern height in the reverse direction from which the material originally flowed into the mold. Factors that influence this residual stress include the relative molecular mass or viscosity of the resist and the amount of time the pattern is annealed at high temperature in the presence of the mold. © *2006 American Vacuum Society.*
[DOI: 10.1116/1.2387157]

I. INTRODUCTION

Nanoimprint lithography (NIL) is emerging as a versatile next generation lithography. The technique receives significant attention because of its combination of high patterning resolution in a low cost tool. Examples of this resolution are seen by reports that feature even smaller than 10 nm can be patterned with imprint processes, approaching a molecular scale resolution.[1,2] This is exciting because NIL has the potential to pattern not just specialized resist formulations for pattern transfer, but also a range of polymeric or soft materials that may have structural, chemical, electrical, or optical functionality. Because of this generality and low cost, NIL has the potential to make state-of-the-art nanoscale patterning a reality for sectors extending beyond the semiconductor industry.

The high resolution of NIL patterning also raises serious concerns with respect to the stability of the imprinted features. One can imagine that a freestanding polymer nanostructure might also be very unstable. Factors such as surface tension and finite size effects become very significant when the pattern size reaches the nanoscale. For example, planar polymer films sometimes spontaneously dewet when their thickness is reduced to tens of nanometers.[3–7] Nanostructures produced by chemically amplified photoresists show an increased propensity for pattern collapse as the their width decreases below 100 nm.[8] Likewise there are simulations indicating a strong reduction in the fundamental elastic moduli of the material inside a nanostructure when the width of the nanostructure decreases below 50 nm.[9] These stability concerns are magnified in light of the shear fields generated when a viscous material flows past a rigid surface. The surface area in a NIL mold can be enormous with essentially all the material that flows into the mold being classified as "interfacial." This means that the entire structure is subjected to these large shear fields during the imprint and there may be the potential to lock in nonequilibrium material configurations.

The goal of this article is to illustrate the existence of large residual stresses that are induced by the large shear fields associated with the imprint process, particularly pertains to the thermal embossing form of nanoimprint lithography. The topic of photocurable imprints where the resist fills the mold as a liquid with a waterlike viscosity will be addressed at a later date. Parallel line space gratings with an approximate linewidth of 100 nm are imprinted into a range of polymer films. The precise shape or cross section of these imprints is characterized nondestructively through a combination of critical dimension small angle x-ray scattering[10–13] (CD-SAXS) and specular x-ray reflectivity (SXR).[14–16] To perceive the presence of the processing induced stresses, the samples are heated to temperatures near the glass transition (T_g) of the polymer, where stress relaxation mechanisms are accelerated but the viscous flow mechanisms are still sluggish. The shape of the imprinted pattern is then monitor as a function of annealing time using the CD-SAXS and SXR techniques. The relaxation of the large processing induced stresses is manifested as a change of the pattern shape.

[a)]Author to whom correspondence should be addressed; electronic mail: csoles@nist.gov

II. EXPERIMENT

Large area imprint molds with parallel line and space gratings were fabricated by interference lithography. The patterns in these molds were etched into silicon oxide and all had approximate 100 nm linewidths. We have a variety of these molds with small variations in the linewidth, pitch, height, and sidewall angle; not all of the patterns in this article originate from the same mold. However, the comparisons within each figure below are limited to samples originating from the same mold. The molds were treated with tridecafluoro-1,1,2,2 (tetrahydroctyl)trichlorsilane vapor to create a low-energy self-assembled monolayer that facilitates pattern release. The imprints were made into three different materials. These included two different poly(methylmethacrylate)s (PMMA) with relative molecular masses of 15 and 1000 kg/mol, poly(styrene) with a molecular mass of 96 kg/mol, and the commercial Nanonex 1020 resist formulation (Certain commercial materials and equipment are identified in this paper in order to specify adequately the experimental procedure. In no case does such identification imply recommendation by the National Institute of Standards and Technology nor does it imply that the material or equipment identified is necessarily the best available for this purpose.) The PMMA were dissolved in anisole at concentrations of 6.4% by mass (15 kg/mol) and 2.5% by mass (1000 kg/mol). Poly(styrene) (PS) was dissolved in toluene at a concentration of 4.0% by mass. The films were spun cast at 209 rad/s (2000 rpm) onto Si wafers with a native oxide surface. The spun cast films were baked under vacuum for 30 min at 170 °C for the PMMA and PS and at 80 °C for the Nanonex 1020 resist to remove the residual solvent. The initial film thickness of all samples was deliberately designed to be around 280 nm to minimize the substrate effect. The imprints were made on a Nanonex 2000 imprint tool with a mold that has a pitch of 355 nm for PMMA and 194 nm for both PS and Nanonex 1020 resist. After sufficiently evacuating the sample chamber, the imprints were made in two steps: 10 s at 130 °C and 1.4 MPa (for all films) followed by 10 min at 170 °C and 3.4 MPa for the PMMA, 5 min at 170 °C and 3.4 MPa for the PS, and 1 min at 130 °C and 1.7 MPa for the Nanonex 1020. The imprint tool then was cooled to 55 °C, below the glass transition temperature of the resist, before releasing the pressure and separating the pattern from the mold. The residual layer thickness is measured by SXR to be around 200 nm for PMMA patterns, 125 nm for PS patterns, and 127 nm for the Nanonex resist patterns.

SXR measurements were performed on a Phillips X'pert diffractometer with a θ-2θ configuration. Details of the SXR measurements can be found in Refs. 14–16. For all of the reflectivity data presented here, the mold and the imprinted pattern were adjusted so that the line orientation was perpendicular to the plane defined by the surface normal and the incident beam. However, parallel orientations were also measured and the results are nearly identical to the perpendicular configuration reported here. SXR is a well-established technique for measuring the thickness, density, and roughness of thin films supported on a smooth substrate. Recently we have shown how this technique can also be used to quantify the residual layer thickness, pattern height, and pattern cross section as a function of height.[14–16]

Details of the CD-SAXS technique are described elsewhere.[10–13] Briefly, the technique uses transmission small angle x-ray scattering through the supporting Si wafer, treating the polymer pattern as a diffraction grating. The diffraction peak spacing is given by $\Delta q = 2\pi/L$, where L is the pattern period, $q = 4\pi/\lambda \sin(\theta)$, λ is the x-ray wavelength, and 2θ is the scattering angle as measured along the axis of diffraction. Parameters describing the pattern cross section are determined by the relative intensity of the peaks at varying angles of incidence ω, with $\omega = 0°$ defined as the incident beam normal to Si wafer.[10–13] The CD-SAXS measurements were performed at the Advanced Photon Source at Argonne National Laboratory. The key to the technique is to use an x-ray energy that is just below the absorption edge of Si, enabling transmission scattering through the supporting Si wafer. Selecting an x-ray wavelength of 1 Å or less, which is easily done at a synchrotron source, achieves this condition (it is also possible to do transmission scattering using a Mo K_α x-ray source in a laboratory x-ray generator).

III. RESULTS

The patterns imprinted into the 15 kg/mol PMMA were characterized at room temperature using the CD-SAXS technique. The as-imprinted patterns were fully characterized at room temperature over $-20° \leqslant \omega \leqslant +20°$ in increments of $(1 \pm 0.05)°$; collecting data over this angular range required about 80 min. The scattering data were fitted to a trapezoidal cross section for the lines with an average linewidth W of 141 ± 1 nm, an average height H of 210 ± 10 nm, and an average sidewall angle β of $5° \pm 0.5°$. To determine the validity of the trapezoid model requires collecting data over such a large ω range. Once the pattern shape was completely characterized at room temperature the sample temperature was increased to about 101 °C, 15 °C above the T_g of the PMMA, and held *in situ* in the x-ray beam. Over the period of 80 min required to collect the entire ω rotation from $-20°$ to $+20°$ the pattern changes significantly for temperatures near T_g, making *in situ* rotation measurements unfeasible. Therefore the *in situ* changes in the diffraction pattern were recorded only at the normal incidence condition of $\omega = 0°$. These data sets could be collected in approximately 2 min intervals. The full ω rotation of $\pm 20°$ is needed initially to determine the correct model, for example, the trapezoid here. However, if the shape of the model does not change significantly (e.g., the trapezoid does not turn into hemispherical drop) with annealing, the changes in the fitting parameters for just the normal incidence scattering data are sufficient to extract the changes in the model dimensions. For the annealing times and temperatures employed here, we have confirmed that the trapezoidal cross section is a reasonable approximation throughout the annealing process.

In the case of imprinted 15 kg/mol PMMA patterns, after annealing the lines for 46 min near $T_g + 15$ °C, the line shape

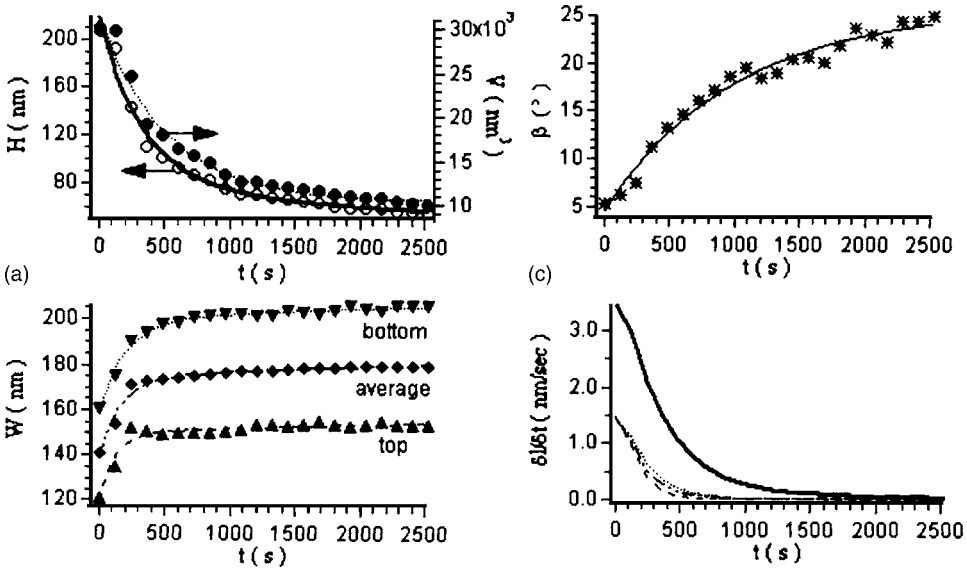

FIG. 1. Time dependence of the different trapezoid parameters is shown while annealing the 15 kg/mol PMMA patterns at approximately T_g +15 °C. Part (A) shows the decrease in both the pattern height H (open symbols) and volume of material in the patterns (closed symbols) derived from the scattering intensity. Parts (B) and (C) show the corresponding increase in the width W and sidewall angle β over the same period. Part (D) compares the rate of change for H (heavy solid line) and the different W's (thin lines) for by taking the derivative of the arbitrary smooth functions fit to the experimental data in parts (A) and (B). The error bars indicate the standard uncertainty of the different trapezoid shape parameters.

evolved into a trapezoid with an average linewidth W of 180 ± 1 nm, an average height H of 55 ± 10 nm, and an average side-wall angle β of $25°\pm0.5°$; the trapezoids decrease in height and broaden in width. The time evolution of this shrinking and broadening processes, or pattern decay, of the 15 kg/mol PMMA imprint is shown in Fig. 1. These data were recently introduced elsewhere[17] and discussed in greater detail here. The time dependence curves in Fig. 1 show that the decay of the PMMA patterns is initially fast but slows down markedly at longer times. In parts (A)–(C) an arbitrary smooth exponential function is fitted to the data. Part (D) shows the derivative of this fit function for the H and W dependencies. What is striking is that in the initial stages of decay in the pattern height are much faster than the rate of pattern broadening. In the early stage of annealing, H decreases at a rate of ≈3 nm/s but this slows to ≈0.01 nm/s at long times (2500 s). By contrast, the rates of pattern width broadening (including the average, top, and bottom widths of the trapezoid) are ≈1 nm/s initially. After 1000 s the linewidth evolution slows down significantly to ≈0.01 nm/s and remains nearly constant at longer times. At 1000 s the decay rate in H is still an order of magnitude greater, ≈0.3 nm/s. While the decay rate in H also reaches a constant on the order of 0.01 nm/s, it does not approach this value until 2500 s; at 1000 s the rate of change in pattern height is still about one order of magnitude greater than the rate of change in pattern width.

Hamdorf and Johansmann[18] and Petersen and Johansmann[19] studied similar pattern decay effects in PMMA surfaces perturbed with much larger wavelength sinusoidal patterns. In their model, surface tension drives the radius of curvature of the sinusoidal corrugations to into a flat surface. They assumed that the polymer acts as a Newtonian fluid with a constant surface tension σ and derived an expression for the change in the pattern height as a function of viscosity η and time t: $dH/dt=(-\pi\sigma H)/(2L\eta)$, where L is the wavelength of the sinusoidal pattern. In their experiments, the decay in pattern height was exponential with t, similar to the form of the decay in Fig. 1. We input our late stage pattern height decay rate into the model of Johannsmann to crudely approximate (because our patterns are clearly not sinusoidal) the polymer viscosity. Taking a reasonable value of $\sigma\approx70$ mN/m for PMMA, we find $\eta\approx1\times10^9$ Pa s when dH/dt approaches a constant value near $t=2500$ s. At earlier times, for example, at $t=1000$ s and $t=100$ s where dH/dt is larger, similar estimates predict smaller viscosities of $\eta\approx1\times10^8$ Pa s and $\eta\approx1\times10^7$ Pa s, respectively. The bulk viscosity of PMMA is approximated using the Williams-Landel-Ferry (WLF) relationship $\eta/\eta_0=C_1(T-T_0)/(C_2+(T-T_0))$, where η_0 ($=1\times10^{12}$ Pa s) and T_0 ($=118$ °C) are a reference viscosity and temperature, and the constants C_1 (=12.21) and C_2 (=70.1) are empirically determined.[20] The WLF predicted viscosity for bulk PMMA is approximately $\eta_{\text{bulk}}=7.9\times10^9$ Pa s. This is clearly more consistent with the dH/dt values after 2500 s of annealing. The late stage pattern evolution appears to approach a surface tension driven viscous flow regime while the early stage decay rate is accelerated.

There are a couple of possible explanations for the accelerated early stage pattern decay rates. Unlike the sinusoidal imprints studied by Johannsmann, it is recognized that the patterns here possess a nonuniform radius of curvature. The small radius of curvature at the vertices of the trapezoid will produce large, localized Laplace pressure gradients that may be responsible for the accelerated flow. To properly model the surface tension driven decay of the pattern, these radii of curvature need to be properly accounted for. Before developing these models, it is not immediately clear how such an effect would lead to an anisotropy in the rates of decay in the height and width directions. This anisotropy would seem to suggest an inherent anisotropy in the material. In the remainder of this article we will experimentally demonstrate that the rapid decay in pattern height relative to pattern width is driven at least partially by residual stresses induced during the imprint process. The large shear fields induce viscoelastic

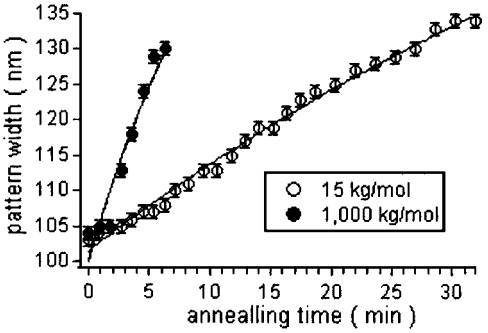

FIG. 2. Changes in the average trapezoid width are shown as a function of annealing time at approximately T_g+10 °C for both 15 kg/mol (open symbols) and 1000 kg/mol (filled symbols) PMMA. The rate of change is faster in the higher molecular mass PMMA, the opposite of what would be predicted by surface tension and viscosity. The error bars indicate the standard uncertainty in the pattern widths and the lines are arbitrary fits drawn to guide the reader's eyes.

distortions of the material during the imprint process, providing an elastic restoring force that dramatically decreases the line height at elevated temperatures.

Our first evidence that residual stress is a dominant factor driving the early stage pattern decay comes from the molecular mass effects on the decay process. For entangled polymers, the surface tension does not vary noticeably with molecular mass; however, the melt state zero shear viscosity scales as $\eta \propto M^{3.4}$, where M is the relative molecular mass. This means that the driving force for pattern decay in the surface tension driven regime of Johannsmann should not change with molecular mass but the kinetic response, dictated by the viscosity, of a low molecular mass polymer pattern should be significantly faster than the high molecular mass analog. To test this hypothesis, identical patterns were imprinted into two different PMMA films, one with a molecular mass of 15 kg/mol and another of 1000 kg/mol. In terms of the zero shear η, the pattern decay rate of the high molecular mass pattern should be $\approx 2\times 10^6$ times slower. Figure 2 compares the time dependence of the pattern width broadening in the two PMMA patterns at T_g+10 °C. The rate of pattern shape change is the *opposite* of what viscosity would predict, larger in the higher molecular mass PMMA. This cannot be rationalized with a simple surface tension effect.

Higher molecular mass PMMA will also have a significantly larger viscosity during the imprint process. This will generate greater shear fields as the viscous material is squeezed into the mold cavity. In fact, it is likely that the mold fill process is accompanied by viscoelastic deformation of the material. This has the potential to induce biases or internal stresses in the material during the nanoimprint process. These biases will be oriented in the direction of material flow, i.e., in the height direction. Both the faster decay of pattern height relative to pattern width and the faster rate of change in the higher molecular mass PMMA imprints are consistent with this internal stress mechanism.

It should also be possible to relax the biases or stresses induced by the imprint process and see their effect on the

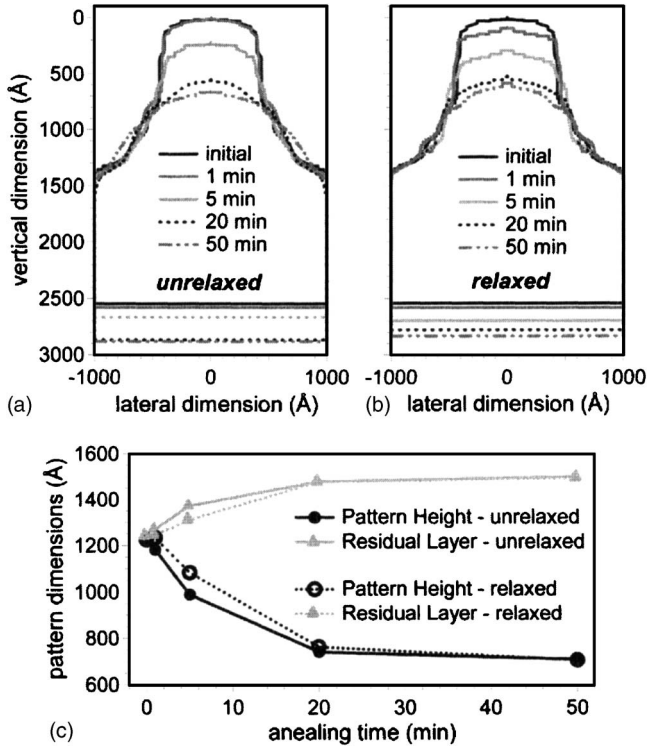

FIG. 3. Parts (A) and (B) shows the changes in the pattern cross sections as a function of annealing time at approximately T_g+5 °C for a 96 kg/mol PS in both the "unrelaxed" and "relaxed" samples, respectively. The estimated standard uncertainty in the profile dimensions is approximately 50 Å. Part (C) emphasizes the changes in the pattern height and the residual layer thickness, illustrating that the dimensions change more quickly in the the unrelaxed state. Error bars indicate the standard uncertainty in the heights.

kinetics of the pattern decay. To illustrate this, two imprints were made into a PS film with a molecular mass of 96 kg/mol using identical imprint times, temperatures, and pressures. After imprinting and cooling back to room temperature, the mold was immediately separated from one of the patterns. The mold was left in contact with the pattern for the remaining imprint and annealed in a vacuum oven at 170 °C for 27 h. At 70 °C above T_g the PS should have enhanced mobility to help relax the stresses induced by the imprint process. After annealing for 27 h, the sample was cooled to room temperature and the mold was separated from the imprint. In this case the decay of the "relaxed" and "unrelaxed" imprints were characterized by SXR. SXR is inherently slower than CD-SAXS, requiring approximately 1 h for each measurement. This means that each sample had to be annealed on an external hot plate for sequential intervals of time with the SXR data collected between each interval at room temperature; *in situ* measurements are not possible with SXR. However, SXR has the added benefit that it can simultaneously quantify the residual layer thickness. Up to now the role of the residual layer in the pattern decay process has not been addressed.

Figure 3 shows the time dependence of the pattern height decrease at T_g+5 °C for both the relaxed and unrelaxed imprints. Parts (a) and (b) show how the complete pattern profiles change with annealing while part (c) emphasizes the

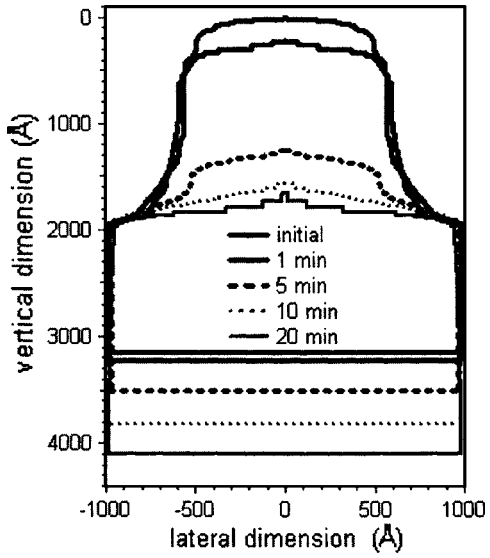

FIG. 4. Changes in pattern cross section are shown as a function of annealing time at 70 °C for the Nanonex 1020 commercial imprint resin. Notice how the pattern decreases in height more dramatically than it broadens in width, especially for the shorter annealing times. The estimated standard uncertainty in the profile dimensions is approximately 50 Å.

changes in pattern height and residual layer thickness. As expected, annealing the imprint inside the mold at elevated temperatures helps to partially relax the residual stresses in the imprint and retard the decay process. For a given annealing time, the amount of change in the relaxed structures was less than the unrelaxed. The effect is small but noticeable and it remains to be seen how long the sample needs to be annealed to completely relax the stresses. One can also see that the residual layer thickness increases as the pattern decays in height. A simple first order approximation reveals that the volume of the material lost by the pattern in terms of just the height decay equals the volume of material gained by the residual layer thickness increase. This important observation is consistent with the minimal change in pattern width during the decay. A loss in height does not correspond to an increase in width; a loss in height shows up as an increase of the residual layer thickness. Notice that retarded kinetics of the pattern height decay in the relaxed sample is also mirrored in the growth of the residual layer.

The processing induced residual stress appears to be a general phenomenon for the thermal form of imprinting. PS and PMMA are model polymer systems but the effect is also seen in commercial imprint formulations. An example of this is shown in Fig. 4 where the time dependent evolution of a pattern imprinted into a Nanonex 1020 commercial imprint is shown. The evolution of the complete line shape profiles extracted from SXR data is overlaid for various annealing times at 70 °C. For this commercial resist formulation, we do not know the exact T_g. Nevertheless, once again the pattern decays primarily in height with little change in the width. Compared to PS and PMMA the anisotropy is not as pronounced, but the general phenomena are similar. Only at longer annealing times is there evidence of broadening.

The notion of process induced nanoimprinting stresses is not without precedent. Here we characterize the stability of the protrusions in the imprinted pattern, which is the regions where material flows into the cavity of the mold. There are a few complimentary studies focusing on the recesses in the pattern that correspond to the protrusions in the mold. These are the regions depleted of material when the mold is pressed into the film, that is, regions corresponding to the residual layer. There are often reports of an elastic recovery of these depressed regions manifest as a local increase in the thickness of the residual layer after demolding. This also suggests that there are elastic stresses stored in the material after imprinting.[21–23] This is also consistent with developing notion that during the imprint process the viscous flow approaches the shear thinning regime;[23,24] high rates of shear would be needed to induce stresses. More recently there was also a report by Johannsmann on the decay of shallow (0.8 nm) grating patterns with a periodicity in the range of 25–60 nm.[25] They observed pattern decay at temperature of 30 °C below the bulk T_g of the polymer. This was interpreted as evidence for a depressed surface T_g of the polymer. While the amplitude of these patterns was not particularly large, it is also possible that this accelerated decay reflects imprinting induced stresses.

Applications that utilize the thermal embossing form of NIL need to be aware of these internal stresses and their potential impact on the intended function of the imprinted pattern. This will become increasingly important as the feature sizes that are imprinted continue to shrink and the materials that are imprinted move away from resist formulations that are sacrificial, i.e., do not have to remain stable for very long periods of time. Most high-resolution commercial imprint formulations are photocurable, low-viscosity liquids where shear-induced stresses would seemingly be minimized (although we have not addressed these systems yet). However, functional materials that might be patterned into a device may not be amenable to phtotocurable imprints; thermal embossing may be the only recourse. With respect to the commercial thermal imprint resists, there is the notion that the imprint temperature should be close to room temperature to minimize the heating of the substrate. To minimize thermal distortions, coefficient of thermal expansion mismatch issues, and shrinkage upon cooling, this approach is logical. However, room temperature imprint resists will also have a greater propensity to relax their shear-induced stresses at room temperature and possibly lead to major long-term stability issues. For many applications a pattern that changes its shape as a function of time will be of little use. The issue of imprint-induced stresses also needs to be considered from the perspective of cohesive strength. There are reports showing that when imprinting very small features with a high aspect ratio high molecular mass polymers are superior in their cohesive strength; the low molecular mass analogs have a greater propensity to shear off during mold separation.[26] The observations here illustrate that the increased cohesive strength will also be accompanied by increased levels of residual stress. In certain applications this may or may not be

important. A final example of where residual stresses need to be considered is in the use of thermal reflow techniques. In chemically amplified photoresists thermal reflow techniques are often used to reduce line edge roughness. The pattern is flash annealed above the T_g of the resist where surface tension effects can smooth out feature roughness without significantly changing the overall pattern shape. As we have shown here, the residual stresses can dominate over surface tension during these flash annealings which may lead to dramatic shape changes. This is especially important if the combination of NIL plus thermal reflow is used to fabricate microlenselet arrays. Understanding how the residual stress impacts the reflow response will be critical to engineering the shape of the microlene.

IV. CONCLUSIONS

The thermal embossing form of NIL produces large shear stresses as the viscous polymer melt is forced into the nanoscale cavities of the mold. These stresses do not completely relax during the imprint process and are locked into the resulting structures as they were cooled into the glassy state. Once the mold is separated from the imprint, these process induced residual stresses have the propensity to relax, especially at elevated temperatures, through an anisotropic and irreversible pattern shape change. The patterns decrease in height faster than they broaden in width, displaying a memory of the original flow patterns when the mold was filled. The levels of residual stress can be reduced by either annealing at elevated temperatures in contact with the mold for extended periods of time or using a low molecular mass resist that has a lower viscosity.

ACKNOWLEDGMENTS

The authors acknowledge the NIST Office of Microelectronics and the ATP Intramural Funding Program for their financial support and the Nanonex Corporation for their assistance in fabricating the imprint patterns. The Advanced Photon Source, where the CD-SAXS measurements are performed, is supported by the U.S. Department of Energy under Contract No. W-31-109-Eng-38. Stella Pang and Ronald Reano helped by imprinting the patterns used in Fig. 1.

[1]M. D. Austin, H. Ge, W. Wu, M. Li, Z. Yu, D. Wasserman, S. A. Lyon, and S. Y. Chou, Appl. Phys. Lett. **84**, 5299 (2004).
[2]F. Hua *et al.*, Nano Lett. **4**, 2467 (2004).
[3]G. Reiter, Phys. Rev. Lett. **68**, 75 (1992).
[4]J. Bischoff, D. Scherer, S. Herminghaus, and P. Leiderer, Phys. Rev. Lett. **77**, 1536 (1996).
[5]R. Xie, A. Karim, J. F. Douglas, C. C. Han, and R. Weiss, Phys. Rev. Lett. **81**, 1251 (1998).
[6]K. Jacobs, S. Herminghaus, and K. R. Mecke, Langmuir **14**, 965 (1998).
[7]D. B. Hall, J. C. Hooker, and J. M. Torkelson, Macromolecules **30**, 667 (1997).
[8]H. B. Cao, P. F. Nealey, and W.-D. Domke, J. Vac. Sci. Technol. B **18**, 3303 (2000).
[9]K. Van Workum and J. J. de Pablo, Nano Lett. **3**, 1405 (2003).
[10]R. L. Jones, T. J. Hu, E. K. Lin, W.-L. Wu, R. K. Kolb, D. M. Casa, P. Boulton, and G. G. Barclay, Appl. Phys. Lett. **83**, 4059 (2003).
[11]T. J. Hu, R. L. Jones, E. K. Lin, W.-L. Wu, D. Keane, S. Weigand, and J. P. Quintana, J. Appl. Phys. **96**, 1983 (2005).
[12]R. L. Jones *et al.*, Proc. SPIE **5751**, 415 (2005).
[13]R. L. Jones *et al.*, J. Microlithogr., Microfabr., Microsyst. **5**, 013001 (2005).
[14]H.-J. Lee, C. L. Soles, H. W. Ro, D. R. Hines, R. L. Jones, E. K. Lin, and W.-L. Wu, Proc. SPIE **5751**, 1203 (2005).
[15]H.-J. Lee, H. W. Ro, C. L. Soles, R. L. Jones, E. K. Lin, W. Wu, and D. R. Hines, J. Vac. Sci. Technol. B **23**, 3023 (2005).
[16]H.-J. Lee, C. L. Soles, H. W. Ro, D. R. Hines, R. L. Jones, E. K. Lin, and W.-L. Wu, Appl. Phys. Lett. **87**, 263111 (2005).
[17]R. L. Jones, T. Hu, C. L. Soles, E. K. Lin, R. M. Reano, S. W. Pang, and D. M. Casa, Nano Lett. **6**, 1723 (2006).
[18]M. Hamdorf and D. Johannsmann, J. Chem. Phys. **112**, 4262 (2000).
[19]K. Petersen and D. Johannsmann, J. Non-Cryst. Solids **307**, 532 (2002).
[20]D. J. Plazek, V. Tan, and V. M. O'Rourke, Rheol. Acta **13**, 367 (1974).
[21]C. Martin, L. Ressier, and J. P. Peyrade, Physica E (Amsterdam) **17**, 523 (2003).
[22]G. W. L. Cross, B. O'Connell, and J. B. Pethica, Appl. Phys. Lett. **86**, 081902 (2005).
[23]H. Schultz, M. Wissen, N. Bogdanski, H.-C. Scheer, K. Mattes, and Ch. Friedrich, Microelectron. Eng. **83**, 259 (2006).
[24]H. D. Rowland and W. P. King, J. Micromech. Microeng. **14**, 1625 (2004).
[25]E. Buck, K. Petersen, M. Hund, G. Krausch, and D. Johannsmann, Macromolecules **37**, 8647 (2004).
[26]Y. Hirai, S. Yoshida, N. Takagi, Y. Tanaka, H. Yabe, K. Sasaki, H. Sumitani, and K. Yamamoto, Jpn. J. Appl. Phys., Part 1 **42**, 3863 (2003).